How to observe and quantify quantum-discorded states

Matthew A. Hunt,[1] Igor V. Lerner,[1] Igor V. Yurkevich,[2] and Yuval Gefen[3]

[1]*School of Physics & Astronomy, University of Birmingham, B15 2TT, UK*
[2]*School of Engineering & Applied Science, Aston University, Birmingham B4 7ET, UK*
[3]*Department of Condensed Matter Physics, The Weizmann Institute of Science, Rehovot 76100, Israel*

Quantum correlations between parts of a composite system most clearly reveal themselves through entanglement. Designing, maintaining, and controlling entangled systems is very demanding, which raises the stakes for understanding the efficacy of entanglement-free, yet quantum, correlations, exemplified by *quantum discord*. Discord is defined via conditional mutual entropies of parts of a composite system, and its direct measurement is hardly possible even via full tomographic characterization of the system state. Here we design a simple protocol to detect quantum discord and characterize a discorded state in an *unentangled* bipartite system. Our protocol is based on an electronic setup and relies on a characteristic of discord that can be extracted from repeated direct measurements of current correlations between subsystems. The proposed protocol opens a way of extending experimental studies of discord to many-body condensed matter systems.

While quantumness of correlations between the parts of a system in a pure state is fully characterized by their entanglement (see Ref. 1 for reviews), mixed states may possess quantum correlations even if they are not entangled. The quantumness of the correlations is properly described in terms of quantum discord [2, 3][4] which is a discrepancy between quantum versions of two classically equivalent expressions for mutual entropy in bipartite systems (see Ref. [5–7] for reviews). Any entangled state of a bipartite system is discorded, but discorded states may be non-entangled. Although it is entanglement which is usually assumed to be the key resource for quantum information processes, it was suggested that quantum enhancement of the efficiency of data processing can be achieved in deterministic quantum computation with one pure qubit which uses mixed *separable* (i.e. non-entangled) states [8–11]. In such a process, which has been experimentally implemented [12], the nonclassical correlations captured by quantum discord are responsible for computational speedup [13]. Quantum discord was also shown to be the necessary resource for remote state preparation [14], and for the distribution of quantum information to many parties [15, 16]. Unlike entanglement, discord is rather robust against decoherence [17]. Thus, along with entanglement, quantum discord can be harnessed for certain types of quantum information processing.

Despite increasing evidence for the relevance of quantum discord, *quantifying* it in a given quantum state is a challenge. Even full quantum state tomography would not suffice, since determining discord requires minimizing a conditional mutual entropy over a full set of projective measurements. An alternative, geometric measure of discord [18–21] has been successfully implemented experimentally [22–24]. However, geometric discord also faces serious problems. For example, it can increase, in contrast to the original quantum discord, even under trivial local reversible operations on the passive part of the bipartite system [25] (note, though, the proposal of Ref. [26] to mend this deficiency). Most seriously, being a non-linear function of the density matrix ρ, geometric discord can only be quantified via (full or partial) reconstruction of ρ itself. This severely limits its susceptibility to experiment in the many-body context.

In this Letter we propose a novel discord quantifier which would overcome these fundamental difficulties and render quantum discord to be experiment-friendly for many-body electronic systems, where it has not yet been observed. We present a protocol to detect and characterize quantum discord of any unknown mixed state of a generic *non-entangled* bipartite system, implemented in either electronic or photonic setup. The protocol is based on direct repeated measurements of certain two-point correlation functions (which are linear in ρ as any direct quantum-mechanical observable). While discord cannot be detected by a single linear measurement [6, 27], we show in detail how *repeated* measurements would allow one to both detect a discorded state and build its reliable quantifier.

Below we will focus on describing how to measure discord in a bipartite two-qubit system. After stating a few facts about the latter, we will present an electronic setup, where a bipartite mixed state can be generated. We then define a relevant two-point correlator, by way of which we can detect and quantify discord. We demonstrate our protocol by applying it to a few specific states.

A generic non-entangled bipartite system is described by the density matrix [28]

$$\rho^{AB} = \sum_{\nu=1}^{M} w_\nu \rho_\nu^A \otimes \rho_\nu^B, \qquad (1)$$

where the classical probabilities w_ν add up to 1, and each ρ_ν^X describes a pure state of the appropriate subsystem $(X = A, B)$, so that they can be parameterized as $\rho_\nu^X =$

$|X_\nu\rangle \langle X_\nu|$. It turns out [5, 18, 29] that the mixed state (1) is A-discorded [30] independently of ρ_ν^B, *unless* $\{|A_\nu\rangle\}$ form an orthogonal basis. In order to detect and quantify A-discord, we propose to utilize this property of state (1). To this end, we consider correlation functions that are governed by the conditioned density matrix,

$$\rho^{A|B} = \sum_{\nu=1}^{n} w_\nu^B \rho_\nu^A. \qquad (2)$$

The state described by $\rho^{A|B}$ at the input terminal of subsystem A evolves into an out-state described by density matrix $\widetilde{\rho}^{A|B}$ that can be diagonalised by adjusting experimentally-controlled parameters of A. The coefficients w_ν^B will depend on the probabilities w_ν and details of the evolution of subsystem B to be specified later.

We will show that such adjusted parameters are w_ν^B-independent only if the states $\{|A_\nu\rangle\}$ form an orthogonal basis, i.e. ρ^{AB} has no A-discord. Thus their dependence on w_ν^B is a signature of A-discord. We propose to measure a joint correlation function K of the two subsystems that makes such a dependence visible, and to employ K for quantifying discord. We describe here in detail how to build a reliable discord quantifier based on the correlation function using, for simplicity, a two-qubit bipartite system as an example.

It is well known [6] that a separable state can be prepared by local operations and classical communications. Here we propose a particular way of preparing such a state in a solid state setup. A two-qubit bipartite system with a mixed state, Eq. (1), can be implemented with the help of two Mach-Zehnder interferometers, MZI^B and MZI^A, corresponding to subsystems B and A (cf. Fig. 1). Such a system can be realized as an electron-based setup in a quantum Hall geometry, where the arms of the MZIs are constructed via a careful design of chiral edge modes, and quantum point contacts (QPC) act as effective beam-splitters (BS) [31–33]. It can also be realized as a photonic device using standard interferometry.

Each qubit is in a quantum superposition of up, $|\uparrow\rangle$, and down, $|\downarrow\rangle$, states corresponding to a particle transmitted through the upper or lower arm of the appropriate MZI. The coefficients in each superposition are determined by the gate-controlled transparency/reflection of the appropriate BS, with a phase difference between $|\uparrow\rangle$ and $|\downarrow\rangle$ (ϕ_B, ϕ_A) controlled by the Aharonov–Bohm flux (measured in units of the quantum flux, hc/e).

The mixed state, Eq. (1), can be created with the help of a *classical* computer that simultaneously and randomly switches transparency/reflection of BS_0^B and BS_0^A between n values. The probabilities w_ν in this equation are now proportional to the time of the pair of BS_0 having the appropriate transparencies, provided that the output on the detectors $D_{1,2}^B$ and $D_{1,2}^A$ is averaged over time intervals much longer than the switching time.
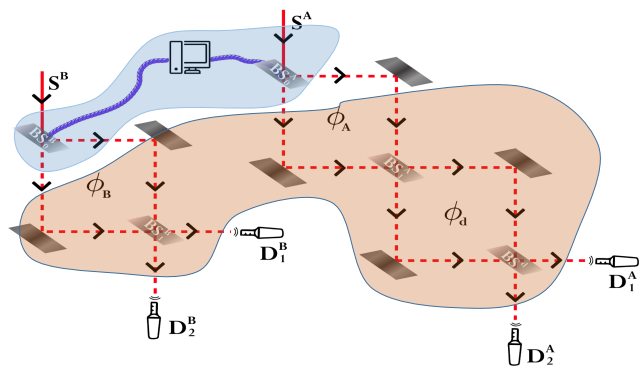
Principal steps of the proposed protocol. Central

FIG. 1. Proposed setup of the bipartite system made of two Mach-Zehnder interferometers, MZI^A with the phase difference ϕ_A, and MZI^B with ϕ_B. The light blue (light brown) area represents the state-preparation (the state evolution and discord measurement) part of the protocol. Electrons from sources S^A and S^B enter beam-splitters BS_0^A and BS_0^B, whose random transparencies are synchronized by a classical computer allowing the creation of mixed states of the form given by Eq. (1). The final state is controlled by transparencies of beam-splitters BS_1^A and BS_1^B and phases $\phi_{A,B}$, and is recorded at any pair of detectors D_i^A and D_i^B (with $i = 1$ or 2). Varying the phase difference ϕ_d in the third, detecting MZI^d, would allow one to identify a state with no A-discord as one for which the interference pattern is suppressed for certain parameters of subsystem A and remains suppressed for any tuning of subsystem B (without adjusting A any further), as illustrated below in Fig. (2).

to it will be measuring quantum interference in a cross-correlation function between the outputs on the detectors attached to subsystems A and B. To this end, we use a third, *detecting* MZI^d, cf. Fig. 1. The ϕ_d-interference pattern vanishes for a set of parameters of subsystem A for which the density matrix $\widetilde{\rho}^{A|B}$ (corresponding to the out-state) becomes diagonal in the up-down basis. This set of parameters of A is independent of the state of B only in the absence of A-discord. Its dependence on B will signify the presence of A-discord and allow us to quantify it.

The interference pattern would be revealed in a cross-correlation function of any two operators, $\mathcal{A}$ and $\mathcal{B}$, corresponding to the output observables in subsystems A and B. We consider the joint probability of particles injected into A and B to be recorded at the detectors D_1^A and D_1^B:

$$K = \text{Tr}\left[\mathsf{P}_A \, \mathsf{P}_B \, \mathsf{S} \, \rho^{AB} \, \mathsf{S}^\dagger\right]. \qquad (3)$$

Here $\mathsf{P}_{A,B} = |\uparrow\rangle\langle\uparrow|$ are the projection operators into detectors $D_1^{A,B}$ in the appropriate space, and the unitary S-matrix, $\mathsf{S} = \mathsf{S}_B \otimes \mathsf{S}_d \, e^{i\phi_d \sigma_3 / 2} \, \mathsf{S}_A$, describes independent evolution of the mixed in-state Eq. (1) through subsystems A, B, and the detecting MZI^d, see Fig. 1. The S-matrices for each MZI are products of those corresponding to the beam-splitter and the phase difference

accumulated on the opposite arms,

$$\mathsf{S}_A = \begin{pmatrix} r_A & t_A \\ -t_A^* & r_A^* \end{pmatrix} e^{\frac{i}{2}\sigma_3\phi_A}, \qquad (4)$$

and similarly for S_B.

Tracing over passive subsystem B reduces the correlation function Eq. (3) to

$$K(\phi_d) = \mathrm{Tr}_A \; e^{\frac{i}{2}\sigma_3\,\phi_d} \; \widetilde{\rho}^{A|B} \; e^{-\frac{i}{2}\sigma_3\,\phi_d} \; \mathsf{A}. \qquad (5)$$

Here $\widetilde{\rho}^{A|B} = \mathsf{S}_A \rho^{A|B} \mathsf{S}_A^\dagger$, and the results of measurements on passive subsystem B are included into the conditioned density matrix $\rho^{A|B}$ of Eq. (2) with $w_\nu^B = w_\nu \, \mathrm{Tr}_B \left[\mathsf{P}_B \mathsf{S}_B \rho_\nu^B \mathsf{S}_B^\dagger \right]$, while $\mathsf{A} = \mathsf{S}_d^\dagger \mathsf{P}_A \mathsf{S}_d$ with S^d being a scattering matrix through beam-splitter BS^d in the detecting MZI^d. Choosing it to be a 50:50 BS makes all the matrix elements of A equal to $\frac{1}{2}$.

Due to interference between the $|\uparrow\rangle$ and $|\downarrow\rangle$ states in MZI^d, correlation function Eq. (5) oscillates with the phase difference ϕ_d, controlled in the condensed-matter implementation by the corresponding Aharonov – Bohm flux. We parameterize it as

$$K(\phi_d) = \mathcal{C} + \left(\mathcal{A}e^{i\phi_d} + \text{c.c.} \right). \qquad (6)$$

This defines the visibility of interference, $\mathcal{V} = |\mathcal{A}/\mathcal{C}|$, which is the difference between max and min values of $K(\phi_d)$, weighted by its average. It vanishes when K becomes ϕ_d-independent. This happens when $\widetilde{\rho}^{A|B}$ in Eq. (5) is diagonal, i.e. $\mathsf{S}_A = \mathsf{S}_0$, the diagonalising matrix for $\rho^{A|B}$.

The final step of the protocol is to check whether S_0 is sensitive to changes in passive subsystem B. Such a sensitivity vanishes only if the density matrix of active subsystem A is built on orthogonal states $\{|A_\nu\rangle\}$ when discord is absent [34]. We will prove the sensitivity to be a reliable discord witness and show how to build a discord quantifier based on it.

Protocol implementation. Experimentally, any in-state, Eq. (1), is *repeatedly* generated in the scheme given in Fig. 1 by random simultaneous changes of transparencies of beam-splitters BS_0^B and BS_0^A with fixed probabilities w_ν. A set of raw data for the generated in-state should be obtained by varying the phase difference, ϕ_d, in the detecting MZI^d and measuring the appropriate particle cross-correlation function, Eq. (3). From this data set, one extracts the visibility, Eq. (6), that is a function of three experimentally controlled parameters, α and ϕ_A, characterizing the scattering matrix S_A, and β characterizing S_B (as the phase difference ϕ_B is always fixed in the proposed protocol).

Fixing also β, one represents the data as lines of constant visibility in the $\alpha - \phi_A$ plane, thus producing the visibility landscape. From this one finds ϕ_0 and α_0 that correspond to zero visibility for this value of β. Repeating this for different values of β, one derives the parametric representation of the zero visibility lines as $\alpha_0(\beta)$ and $\phi_0(\beta)$.

Let us demonstrate how the protocol works using for illustration simple *real* specified states where the zero-visibility points must have $\phi_0 = 0 \bmod(2\pi)$. Hence, $\alpha_0(\beta)$ dependence alone is sufficient for quantifying discord for such states; however, we also exploit[34] $\alpha(\phi_A)$ dependence for the example used below that clearly shows $\phi_0 = 0 \bmod(2\pi)$, as expected. Choosing the in-states defining ρ_ν^A in Eq. (1) to be real superpositions of $|\uparrow\rangle$ and $|\downarrow\rangle$, we parameterize them as $|A_\nu\rangle = \cos\frac{1}{2}\theta_\nu |\uparrow\rangle + \sin\frac{1}{2}\theta_\nu |\downarrow\rangle$, and use a similar parameterization for ρ_ν^B with $\theta_\nu \to \widetilde{\theta}_\nu$. Further choosing these in-states 'symmetric', with $\theta_\nu = \widetilde{\theta}_\nu$, leads to the parameterization $\rho^{AB} = \sum_{\nu=1}^n w_\nu |\theta_\nu\theta_\nu\rangle\langle\theta_\nu\theta_\nu|$, where we put $n=2$. Finally, we parameterize the transmission probabilities in $\mathsf{S}_{A,B}$, Eq. (4), as $|t_A|^2 = \sin^2\frac{1}{2}\alpha$ and $|t_B|^2 = \sin^2\frac{1}{2}\beta$, making the visibility for a given in-state a function of these two parameters.

In Fig. 2, we present the visibility landscape for two different in-states, A-discorded and non-discorded, specified in the figure caption. The dependence $\alpha_0(\beta)$ corresponding to the zero-visibility lines in this landscape reveals a striking difference between the non-discorded and discorded states: the latter shows a strong dependence on β while the former is β-independent; this certainly works not only for the chosen but for generic mixed states.[34]

Discord quantifier. The eye-catching signature of discord in Fig. 2(a) is a high non-monotonicity of the zero-visibility lines, $\alpha_0(\beta)$. By contrast, such lines are straight for the non-discorded state in Fig. 2(b). Note that a π-periodic in α pattern of the zero-visibility lines implies that vertical π-jumps in zero visibility curves happen for non-discorded states. Hence, nearly π-jumps in a zero-visibility curves over a small interval of β, Fig. 3(a), signifies weak sensitivity with respect to changes in the passive subsystem similar to that in curves with a small non-monotonicity over a large interval, Fig. 3(b). To treat both cases on equal footing, we employ the standard deviation of $f_\alpha(\beta) \equiv \cos^2[\alpha_0(\beta)]$ from its average over the period as a quantifier of such a sensitivity, which plays the role of a *discord quantifier*:

$$\Delta_\alpha^2 = \int_0^{2\pi} \frac{\mathrm{d}\beta}{2\pi} \left[f_\alpha(\beta) - \overline{f}_\alpha \right]^2, \quad \overline{f}_\alpha = \int_0^{2\pi} \frac{\mathrm{d}\beta}{2\pi} f_\alpha(\beta). \quad (7)$$

This quantifier gives similar results for the two sets of symmetric in-states in Fig. 3. Both have the density matrix $\rho_\theta^{AB} = \frac{1}{2} \left[|\uparrow\uparrow\rangle \langle\uparrow\uparrow| + |\theta\theta\rangle \langle\theta\theta| \right]$ with different θ. For $\theta = 0$, $\rho^{AB} = |\uparrow\uparrow\rangle \langle\uparrow\uparrow|$ is a pure state with no discord, and likewise discord is absent for $\theta = \pi$ when $\rho_\theta^{AB} \to \frac{1}{2} \left[|\uparrow\uparrow\rangle \langle\uparrow\uparrow| + |\downarrow\downarrow\rangle \langle\downarrow\downarrow| \right]$. Thus, discord is small for ρ_θ^{AB} with θ approaching either 0 or π, cf. Fig. 4.

This suggested quantifier is convenient and, although it is by no means unique, it works remarkably well: its
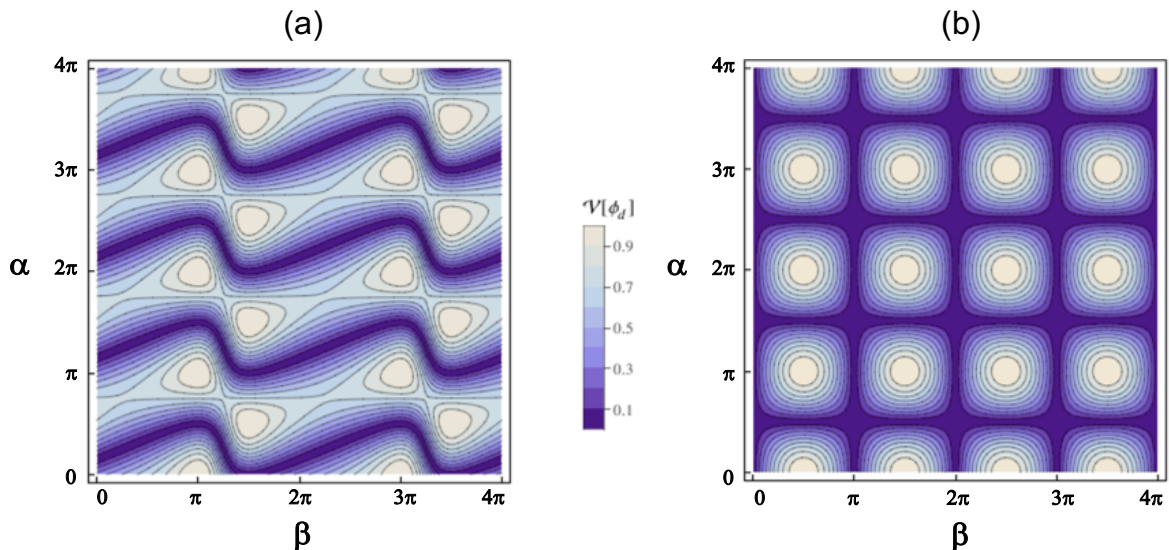
FIG. 2. A striking difference between (a) discorded and (b) non-discorded states: *zero-visibility* (dark) lines are sensitive to changes in the state of passive subsystem B (a) and are independent of this changes in (b). Here we use the symmetric in-states: (a) $\rho^{AB} = \frac{1}{2}\left[\left|\uparrow\uparrow\right\rangle\left\langle\uparrow\uparrow\right| + \frac{1}{2}\left|++\right\rangle\left\langle++\right|\right]$ and (b) $\rho^{AB} = \frac{1}{2}\left[\left|++\right\rangle\left\langle++\right| + \frac{1}{2}\left|--\right\rangle\left\langle--\right|\right]$ with $\left|\pm\right\rangle \equiv \frac{1}{\sqrt{2}}(\left|\uparrow\right\rangle \pm \left|\downarrow\right\rangle)$. Since the states $\left|+\right\rangle$ and $\left|-\right\rangle$ are orthogonal whereas $\left|+\right\rangle$ and $\left|\uparrow\right\rangle$ are not, these density matrices describe a discorded state (a) and a non-discorded state (b), as explained after Eq. (2). Any continuous zero-visibility line in (b) can be chosen for a quantitative characteristic of discord, Eq. (7), cf. Fig. 4.
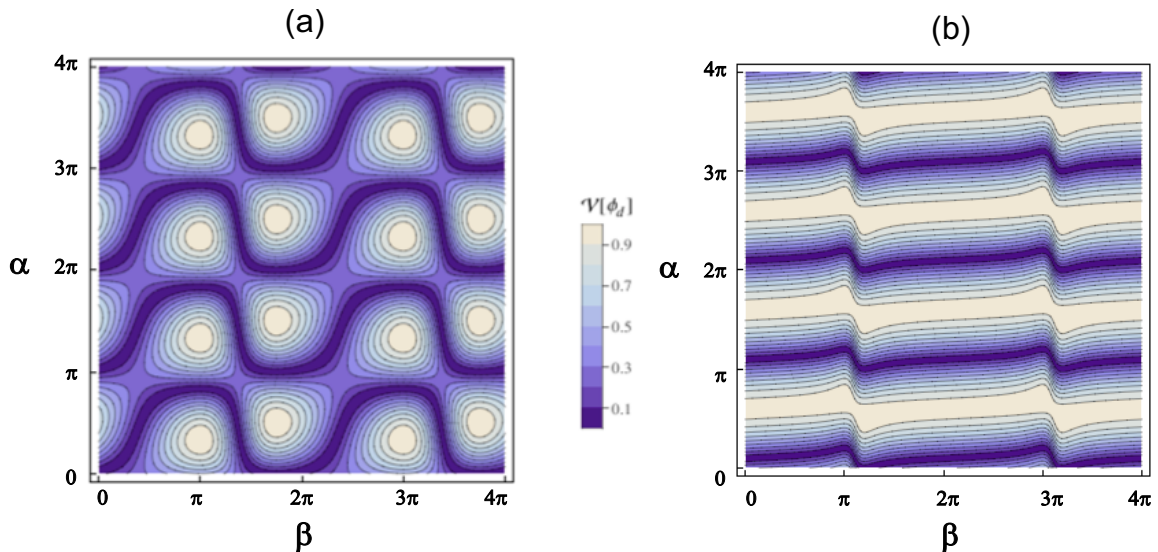

FIG. 3. The visibility plots for $\rho^{AB} = \frac{1}{2}\left|\uparrow\uparrow\right\rangle\left|\uparrow\uparrow\right\rangle + \frac{1}{2}\left|\theta\theta\right\rangle\left\langle\theta\theta\right|$ where in (a) $\theta = \frac{5}{6}\pi$ and in (b) $\theta = \frac{1}{5}\pi$. These density matrices have similar discord, as can be seen from Fig. 4, yet their visibility landscapes look completely different: a π-jump in zero-visibility lines over a small interval of β in (a) signifies weak sensitivity with respect to changes in passive system similar to that in (b) featuring the zero-visibility lines with a small non-monotonicity over a large interval.

similarity to quantum discord in its original definition is quite appealing, as illustrated for ρ_θ^{AB} of the above example in Fig 4. It is straightforward to prove[34] that this measure is reliable: it vanishes for any non-discorded state and does not change with a unitary transformation on passive subsystem B.

Conclusion. We have proposed a new characterization of quantum discord based on measuring cross-correlations in non-entangled bipartite systems and thus

linear in density matrix ρ, in contrast to other quantifiers, notably geometric discord, that require full or partial quantum tomography for reconstruction of ρ. The linearity of the proposed quantifier opens a path to extending experimental research of discord into electronic condensed matter systems. We have considered in detail one possible implementation via devices built of Mach – Zehnder interferometers in quantum Hall systems, where our quantifier is quite robust against external noise and
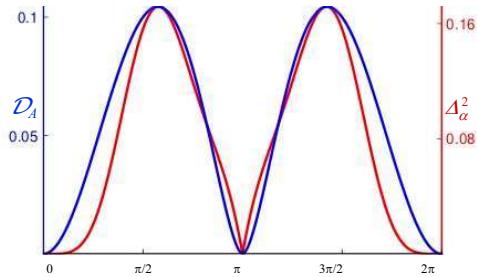
FIG. 4. The standard definition of discord, $\mathcal{D}_A$, (blue) vs the alternative quantifier of Eq. (7), Δ_α^2, (red) for the in-state with the density matrix $\rho_\theta^{AB} = \frac{1}{2}\left[\left|\uparrow\uparrow\right\rangle\left\langle\uparrow\uparrow\right| + \left|\theta\theta\right\rangle\left\langle\theta\theta\right|\right]$.

fluctuations: as long as the Aharonov–Bohm oscillations are resolvable [31], the appropriate interference pattern may serve as a pictorial discord witness, as illustrated above in Figs. 2 and 3. Finally, our discord quantifier is qualitatively consistent, and quantitatively very close to the original measure.

The relative simplicity of this protocol, and the fact that it is based on presently existing measurement technologies and available setups (electronic Mach-Zehnder interferometers) is bound to stimulate experiments in this direction. While the present analysis addresses discord of bi-partite systems, an intriguing generalization of our protocol to multiply-partite systems is possible by introducing a number of coupled interferometers Extension of our protocol to anyon-based states (employing anyonic interferometers) or other topological states may open the horizon to topology-based study of discord.

[1] R. Horodecki, P. Horodecki, M. Horodecki, and K. Horodecki, Rev. Mod. Phys. **81**, 865 (2009).
[2] H. Ollivier and W. H. Zurek, Phys. Rev. Lett. **88**, 017901 (2001).
[3] L. Henderson and V. Vedral, J. Phys. A **34**, 6899 (2001).
[4] For completeness, the full definition of quantum discord[2, 3] is reproduced in *Supplemental Material*.
[5] K. Modi, A. Brodutch, H. Cable, T. Paterek, and V. Vedral, Rev. Mod. Phys. **84**, 1655 (2012).
[6] A. Bera, T. Das, D. Sadhukhan, S. S. Roy, A. Sen(De), and U. Sen, Rep. Prog. Phys. **81**, 024001 (2018).
[7] D. Braun, G. Adesso, F. Benatti, R. Floreanini, U. Marzolino, M. W. Mitchell, and S. Pirandola, Rev. Mod. Phys. **90**, 035006 (2018).
[8] E. Knill and R. Laflamme, Phys. Rev. Lett. **81**, 5672 (1998).
[9] E. Knill, R. Laflamme, and G. Milburn, Nature **409**, 46 (2001).
[10] A. Datta, S. T. Flammia, and C. M. Caves, Phys. Rev. A **72**, 042316 (2005).
[11] H. Cable, M. Gu, and K. Modi, Phys. Rev. A **93**, 040304 (2016).
[12] B. P. Lanyon, M. Barbieri, M. P. Almeida, and A. G. White, Phys. Rev. Lett. **101**, 200501 (2008).
[13] A. Datta, A. Shaji, and C. M. Caves, Phys. Rev. Lett. **100**, 050502 (2008).
[14] B. Dakić *et al.*, Nat. Phys. **8**, 666 (2012).
[15] A. Streltsov and W. H. Zurek, Phys. Rev. Lett. **111**, 040401 (2013).
[16] F. G. S. L. Brandao, M. Piani, and P. Horodecki, Nat. Comm. **6**, 7908 (2015).
[17] L. Mazzola, J. Piilo, and S. Maniscalco, Phys. Rev. Lett. **104**, 200401 (2010).
[18] B. Dakić, V. Vedral, and Č. Brukner, Phys. Rev. Lett. **105**, 190502 (2010).
[19] C. Zhang, S. Yu, Q. Chen, and C. H. Oh, Phys. Rev. A **84**, 032122 (2011).
[20] A. Brodutch and K. Modi, Quantum Info. Comput. **12**, 721 (2012).
[21] D. Girolami and G. Adesso, Phys. Rev. Lett. **108**, 150403 (2012).
[22] R. Auccaise, J. Maziero, L. C. Céleri, D. O. Soares-Pinto, E. R. deAzevedo, T. J. Bonagamba, R. S. Sarthour, I. S. Oliveira, and R. M. Serra, Phys. Rev. Lett. **107**, 070501 (2011).
[23] I. A. Silva, D. Girolami, R. Auccaise, R. S. Sarthour, I. S. Oliveira, T. J. Bonagamba, E. R. deAzevedo, D. O. Soares-Pinto, and G. Adesso, Phys. Rev. Lett. **110**, 140501 (2013).
[24] C. Benedetti, A. P. Shurupov, M. G. A. Paris, G. Brida, and M. Genovese, Phys. Rev. A **87**, 052136 (2013).
[25] M. Piani, Phys. Rev. A **86**, 034101 (2012).
[26] B. Aaronson, R. Lo Franco, and G. Adesso, Phys. Rev. A **88**, 012120 (2013).
[27] R. Rahimi and A. SaiToh, Phys. Rev. A **82**, 022314 (2010).
[28] R. F. Werner, Phys. Rev. A **40**, 4277 (1989).
[29] A. Ferraro, L. Aolita, D. Cavalcanti, F. M. Cucchietti, and A. Acín, Phys. Rev. A **81**, 052318 (2010).
[30] Quantum discord is not necessarily symmetric: one can record discord in one (active) subsystem (A) of a bipartite system while the other (passive) subsystem (B) might be either discorded or not.
[31] Y. Ji, Y. C. Chung, D. Sprinzak, M. Heiblum, D. Mahalu, and H. Shtrikman, Nature **422**, 415 (2003).
[32] E. Weisz, H. K. Choi, I. Sivan, M. Heiblum, Y. Gefen, D. Mahalu, and V. Umansky, Science **344**, 1363 (2014).
[33] H. K. Choi, I. Sivan, A. Rosenblatt, M. Heiblum, V. Umansky, and D. Mahalu, Nat Commun **6**, 7435 (2015).
[34] See *Supplemental Online Materials* for detail.

Supplemental Online Materials

Quantum Discord

Quantum Discord [1,2] exemplifies the difference between classical and quantum correlations of two (sub)systems (A and B), as quantified by mutual information. The latter, which is a classical measure of correlations between A and B, is defined as $I(A:B) \equiv H(A) + H(B) - H(AB)$, where the Shannon entropy $H(A) \equiv -\sum_a p_a \log p_a$ with a being the possible values that a classical variable A can take with the probability p_a, while the joint entropy $H(AB)$ is that of the entire system $A \bigcup B$. An alternative way of writing a classically equivalent expression to $I(A:B)$ is $J(A:B) \equiv H(A) - H(A|B)$, with $H(A|B) \equiv H(AB) - H(B)$ being the conditional entropy which is the uncertainty remaining about A given a knowledge of B's distribution.

The quantum analogues to these expressions can be obtained [1-4] by replacing the Shannon entropies for the probability distributions with the corresponding von Neumann entropies for QM density matrices, $S(\rho) = -\text{Tr}\{\rho \log \rho\}$. The quantum analogue of $I(A:B)$ is then straightforward to define,

$$\mathcal{I}_Q(\rho^{AB}) \equiv S(\rho^A) + S(\rho^B) - S(\rho^{AB}), \tag{S.1}$$

where ρ^A, ρ^B are the reduced density matrices on either subsystem. However, the straightforward analogue to the classical conditional entropy is not that useful since if we defined $S(B|A)$ as $S(A,B) - S(A)$, this quantity would be negative, e.g., in the case when subsystems A and B are in a pure state. Instead, the quantum conditional entropy $S(B|A)$ is defined as the average von Neumann entropy of states of B after a measurement is made on A.

The result of a 'measurement' will depend on the basis we pick for our measurement projectors. Post-measurement density matrix becomes

$$\rho^{AB} \to \sum_\mu p_\mu^A \, \Pi_\mu^A \otimes \rho_{B|\Pi_\mu^A} \tag{S.2}$$

where $\rho_{B|\Pi_\mu^A}$ is the density matrix conditional on some measurement on A as follows,

$$\rho_{B|\Pi_\mu^A} \equiv \frac{1}{p_\mu^A} \, \text{Tr}_A \left(\Pi_\mu^A \otimes \Pi^B \right) \rho^{AB} \left(\Pi_\mu^A \otimes \Pi^B \right) \qquad p_\mu^A = \text{Tr} \left(\Pi_\mu^A \otimes \Pi^B \right) \rho^{AB} \tag{S.3}$$

Using this conditional state, Eq. (S.3), we may extract the entropy $S(\rho_{B|\Pi_\mu^A})$ which gives us the amount uncertainty of the state of B given this projection onto A. We may then obtain the conditional entropy after a complete set of measurements on A, $\{\Pi_\mu^A\}$,

$$S(B|\{\Pi_\mu^A\}) \equiv \sum_\mu p_\mu^A S(\rho_{B|\Pi_\mu^A}) \tag{S.4}$$

From which a generalisation of $J(A:B)$ can be constructed,

$$\mathcal{J}_A(\rho^{AB}) \equiv S(\rho^B) - S(B|\{\Pi_\mu^A\}), \tag{S.5}$$

where one final ingredient has also been added in order to remove the dependence on the measurement basis; we maximised over all complete measurement bases, essentially we pick the *best* measurement basis (that is the one where we are able to reduce our ignorance about subsystem B the most).

Having defined two quantities which would be classically equivalent, the difference between the two could be thought of as a measure of 'quantumness'. This quantity was termed the *quantum discord*,

$$\mathcal{D}_A(\rho^{AB}) \equiv \min_{\{\Pi_\mu^A\}} \left[\mathcal{I}(\rho^{AB}) - \mathcal{J}_A(\rho^{AB}) \right] = \min_{\{\Pi_\mu^A\}} S(B|\{\Pi_\mu^A\}) - \left[S(\rho^{AB}) - S(\rho^A) \right]. \tag{S.6}$$

Note that since $\mathcal{J}$ is not symmetric about which subsystem we perform the measurement on, neither is discord and in general $\mathcal{D}_A(\rho^{AB}) \neq \mathcal{D}_B(\rho^{AB})$.

Derivation of the discord quantifier

In what follows we simulate the visibility data for specified in-states. We will find expressions for zero-visibility lines and show how to construct the visibility landscapes for for any specified non-entangled state. In particular, we illustrate how to do this for the in-states employed in Figs. 2 and 3; we also demonstrate that in this case $\phi_0 = 0 \bmod(2\pi)$, as expected, 6. However, we stress that the known states used for illustrative purposes only: the protocol as described in this section can be experimentally implemented for any non-entangled state.

Visibility for specified in-states. We have defined the visibility $\mathcal{V}$ in terms of the parameters defining correlation function K, Eq. (6). Let us parametrise ρ_ν^A in Eq. (5) via the unit vector on the appropriate Bloch sphere as $\rho_\nu^A = \frac{1}{2}(1 + n_\nu \cdot \sigma) \equiv |n_\nu\rangle\langle n_\nu|$ with

$$n_\nu = (\sin\theta_\nu \cos\phi_\nu, \sin\theta_\nu \sin\phi_\nu, \cos\theta_\nu),$$
$$|n_\nu\rangle = \cos\left(\tfrac{1}{2}\theta_\nu\right)|{\uparrow}\rangle + e^{i\phi_\nu}\sin\left(\tfrac{1}{2}\theta_\nu\right)|{\downarrow}\rangle \tag{S.7}$$

Substituting this into Eq. (2) we obtain the conditioned density matrix in Eq. (5) as

$$\rho^{\mathrm{A|B}} = \tfrac{1}{2}\left[W_B \mathrm{I} + Cn \cdot \sigma\right]$$
$$= \tfrac{1}{2}\left[(W_B - C)\mathrm{I} + C\,|n\rangle\langle n|\right]. \tag{S.8}$$

Here $W_B = \sum_\nu w_\nu^B$, with w_ν^B defined after Eq. (5), and the unit vector $n=(\sin\vartheta\cos\varphi, \sin\vartheta\sin\varphi, \cos\vartheta)$ with the normalisation constant C given by

$$Cn = \sum_\nu w_\nu^B n_\nu. \tag{S.9}$$

State $|n\rangle$ is parameterized via ϑ and φ as in Eq. (S.7):

$$|n\rangle = \cos\tfrac{1}{2}\vartheta\,|{\uparrow}\rangle + e^{i\varphi}\sin\tfrac{1}{2}\vartheta\,|{\downarrow}\rangle. \tag{S.10}$$

From Eq. (S.8) and Eq. (S.10) follows that matrix S_0 that diagonalises $\rho^{\mathrm{A|B}}$ and thus defines zero-visibility lines obeys, up to a phase factor, $\mathsf{S}_0|n\rangle = |{\uparrow}\rangle$ or $|{\downarrow}\rangle$. Using the parameterization of Eq. (4) for $\mathsf{S}_A \to \mathsf{S}_0$, i.e. $|r_0| = |\cos\tfrac{1}{2}\alpha_0|$ and $\phi_A \to \phi_0$, we find that the zero-visibility lines are given by

$$\cos^2\alpha_0 = n_z^2, \quad \text{and} \quad \tan\Phi_0 = -n_y/n_x, \tag{S.11}$$

with $\Phi_0 = \phi_0 + \arg(r_0/t_0)$. More generally, one expresses constant visibility lines, $\mathcal{V} = |\mathcal{A}/\mathcal{C}| = \mathrm{const}$, via the coefficients in Eq. (6) obtained from Eq. (S.8) and Eq. (S.10) as $\mathcal{C} = \frac{1}{2}W_B$ and $\mathcal{A} = \frac{1}{2}\left(c_\uparrow c_\downarrow^*\right)$, with $c_\uparrow = r_A \cos\frac{\vartheta}{2} + t_A \sin\frac{\vartheta}{2}e^{i(\varphi-\phi_A)}$, and $c_\downarrow = -t_A^* \cos\frac{\vartheta}{2} + r_A^* \sin\frac{\vartheta}{2}e^{i(\varphi-\phi_A)}$. For the real in-state used in the example of Fig. 2, we have $\mathcal{C} = \frac{1}{2}\left[1 + \sum_\nu w_\nu \cos(\beta - \theta_\nu)\right]$ and $\mathcal{A} = \frac{1}{4}\sin(\alpha - \vartheta)$, where ϑ is expressible via θ_ν with the help of Eq. (S.9).

Zero-visibility lines for non-discorded states. We now show in detail that the zero-visibility condition is independent of the measurement on B *if and only if* the mixed state ρ^{AB} is non-discorded. The dependence of the measurement on B enters the zero-visibility equation via the coefficients b_ν. This dependence vanishes if all vectors n_ν become parallel to each other, in which case vector n, Eq. (S.9), does no longer depend on coefficients w_ν^B (i.e. sub-system B). This is equivalent to the statement that all states $|n\rangle_\nu$ are either coincide (up to a phase) or orthogonal to each other. In general, states are separated into two mutually orthogonal groups.

As the mutual orthogonality of the in-states $\{|A_\nu\rangle\}$ is a necessary and sufficient condition [4-6] for the mixed state described by the density matrix ρ^{AB}, Eq. (1), to be A-discorded, we have proved that the absence of the β-dependence in the zero-visibility lines signifies the absence of A-discord. Graphically, this leads to horizontal and vertical zero-visibility lines like those in Fig. 2(b). On the contrary, curving zero-visibility lines, as in Figs. 2(a) and 3, give a striking, experimentally accessible signature of quantum discord.

In the above example of applying the protocol, Fig. 2, we have employed the real in-state with $\theta_{B_\nu} = \theta_{A_\nu} \equiv \theta_\nu$ described by the density matrix $\rho^{AB} = \frac{1}{2}|\theta_1\theta_1\rangle\langle\theta_1\theta_1| + \frac{1}{2}|\theta_2\theta_2\rangle\langle\theta_2\theta_2|$. In this case (and for any real in-state), $n_{1y} = n_{2y} = 0$ in Eq. (S.7), so that $\phi_{B_0}=0$ or π. This is clearly seen from the visibility landscape in Fig. 2. This landscape is constructed from Eqs. (S.7) for the two in-states, one with $\theta_1=\pi/2$ and $\theta_2=3\pi/2$, and the other with $\theta_1=0$ and $\theta_2=\pi/2$, both for the fixed $\alpha=\pi/3$. Since the inner product $\langle\theta_1, \theta_2|\theta_1, \theta_2\rangle$ is zero for the first case and non-zero (and $\neq 1$) for the second, these states are, respectively, non-discorded and discorded. This is demonstrated in Fig. 6 where the visibility landscape on the β-α plane shows a striking α-dependence which is a signature of A-discord. The application of the protocol is illustrated by further examples in *Supplemental Material* where the visibility landscape is drawn for a set of further examples, representing the in-states which are asymmetric ($\theta_{B_\nu} \neq \theta_{A_\nu}$), have different probabilities w_ν, non-zero phases, and more than two constituents ($n \neq 2$).
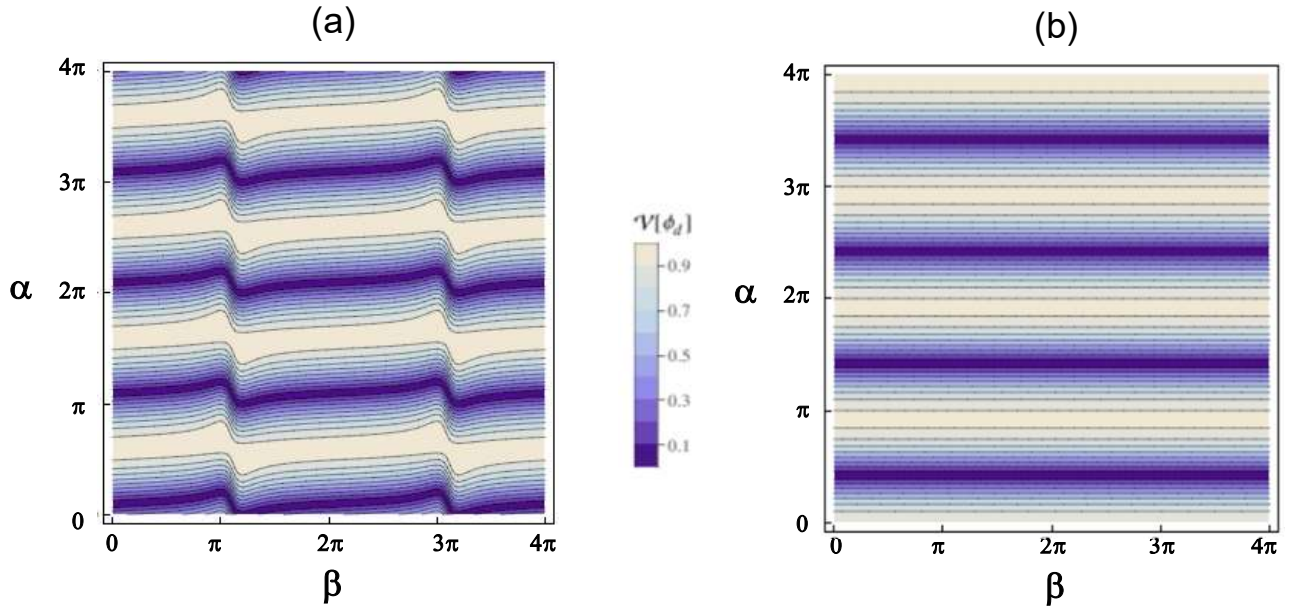
FIG. 5. The visibility plots for (a) $\rho^{AB} = \frac{1}{2}|00\rangle\langle 00| + \frac{1}{2}|+0\rangle\langle+0|$, with $\phi_A = 0$ and (b) $\rho^{AB} = \frac{1}{5}|--\rangle\langle--| + \frac{4}{5}|++\rangle\langle++|$. (a) display the 'grid-like' visibility characteristic of a density matrix which is correlated between A and B subsystems, but undiscorded i.e the correlations are classical only. The barcode graph of (b) is a result of a density matrix which is completely uncorrelated between A and B subsystems. ϕ_A has been fixed as $\phi_{A_0} = 0$ in both plots.

Zero Discord: Grid or Barcode

We demonstrated above that a lack of dependence on β of the lines of zero visibility (i.e the lines are straight as a function of β) means zero discord, but often in cases of zero discord we also see the emergence of vertical straight lines (zero's of visibility which are α independent). We find that the two scenarios of just horizontal lines (barcode) or a grid-like scenario (where both vertical and horizontal zero visibility lines are present) whilst both referring to zero discord states refer to two different routes of getting there. Horizontal lines mean the two subsystems are entirely uncorrelated, whilst grid-like means the two subsystems are correlated but only classically.

Grid-like. A gridded graph such as Fig. 5(a), as well as one of Fig. 8(a), is produced when the state is *classically correlated*, that is when no information about the correlations between subsystems A and B is lost when one makes the correct choice of measurement on subsystem-B.

A classically correlated state (with respect to measurement on A), means that the state described by ρ_1^A is orthogonal to that described by ρ_2^A. States of this form may always be reduced to a mixed state of the form $\sum_{i=1}^2 w_\nu \rho_\nu^A \otimes \rho_\nu^B$, where ρ_ν^A are pure but ρ_ν^B are, in general, mixed and not equal ($\rho_1^B \neq \rho_2^B$). If $\rho_1^B = \rho_2^B$, ρ^{AB} is uncorrelated and we obtain the barcode images in the next part of this section.

The complex amplitude of the oscillatory part of the correlation function was defined in the main text,

$$\mathcal{A} = \left[\mathsf{S}_A \, \rho^{A|B} \, \mathsf{S}_A^\dagger \right]_{12} A_{21}, \tag{S.12}$$

where

$$\rho^{A|B} = \sum_\nu w_\nu^B \, \rho_\nu^A, \quad \mathsf{A} = \mathsf{S}_d^\dagger \, \mathsf{P}_d \, \mathsf{S}_d, \quad w_\nu^B = w_\nu \, \mathrm{Tr}_B \, \rho_\nu^B \mathsf{S}_B^\dagger \, \mathsf{P}_B \, \mathsf{S}_B. \tag{S.13}$$

Assuming the simplest model of the detector QPC,

$$\mathsf{S}_d = \frac{1}{2} \begin{pmatrix} 1 & 1 \\ -1 & 1 \end{pmatrix}, \quad \mathsf{A} = \frac{1}{4} \begin{pmatrix} 1 & 1 \\ 1 & 1 \end{pmatrix}, \tag{S.14}$$

and parametrising A-states as

$$\rho_\nu^A = \frac{1}{2} \left[1 + \mathbf{n}_\nu \, \sigma \right] \tag{S.15}$$

the complex amplitude is written as:

$$\mathcal{A} = \frac{1}{8}\,\mathbf{N}\,\left[\mathsf{S}_A\,\sigma\,\mathsf{S}_A^\dagger\right]_{12}\,, \quad \mathbf{N} = \sum_\nu w_\nu^B\,\mathbf{n}_\nu\,. \tag{S.16}$$

The parametrisation of S_A as

$$r_A = e^{i\varphi_r}\,\cos\frac{\alpha}{2}\,, \quad t_A = e^{i\varphi_t}\,\sin\frac{\alpha}{2}\,, \quad \varphi_\pm = \varphi_r \pm \varphi_t\,, \tag{S.17}$$

with the use of

$$\left[\mathsf{S}_A\,\sigma\,\mathsf{S}_A^\dagger\right]_{12} = \left(r_A^2 - t_A^2,\ -i(r_A^2 + t_A^2),\ -2r_A t_A\right)\,, \tag{S.18}$$

leads to another representation

$$\mathcal{A} = e^{i\varphi_+}\frac{1}{8}\mathbf{N}\mathbf{a}\,, \quad \mathbf{a} = \mathbf{a}_1 + i\mathbf{a}_2\,. \tag{S.19}$$

The complex vector $\mathbf{a}$ is a linear combination of two orthonormal vectors

$$\mathbf{a}_1 = (\cos\alpha\,\cos\varphi_-\,,\cos\alpha\,\sin\varphi_-\,,-\sin\alpha)\,, \tag{S.20}$$
$$\mathbf{a}_2 = (\sin\varphi_-\,,-\cos\varphi_-\,,0)\,, \tag{S.21}$$

The only dependence on B-system may emerge in the vector $\mathbf{N}$ through the coefficients w_ν^B in the linear combination. Writing all vectors in spherical system of coordinates

$$\mathbf{n} = (\sin\theta\cos\phi\,,\sin\theta\sin\phi\,,\cos\theta)\,, \quad \mathbf{N} = N\,\mathbf{n}\,, \tag{S.22}$$
$$\mathbf{n}_\nu = (\sin\theta_\nu\cos\phi_\nu\,,\sin\theta_\nu\sin\phi_\nu\,,\cos\theta_\nu)\,, \tag{S.23}$$

In a general situation, the condition of vanishing oscillations is the orthogonality of vector $\mathbf{N}$ to the set of orthonormal vectors $\mathbf{a}_1$ and $\mathbf{a}_2$. It means that vector $\mathbf{N}$ is parallel to

$$\mathbf{a}_3 = [\mathbf{a}_2 \times \mathbf{a}_1] = (\sin\alpha\cos\varphi_-\,,\sin\alpha\sin\varphi_-\,,\cos\alpha)\,. \tag{S.24}$$

This statement can be written as

$$\mathbf{n} = \pm\mathbf{a}_3\,, \tag{S.25}$$

or, cf Eq. (S.22), in the following form:

$$\alpha = \theta \quad \mathrm{mod}\ \pi\,, \tag{S.26}$$
$$\varphi_- = \phi \quad \mathrm{mod}\ 2\pi\,. \tag{S.27}$$

The angles θ and ϕ may depend on B-system through the coefficients w_ν^B in the linear combination, Eq. (S.16).

NB The solution Eq. (S.25) can be written only for non-zero vectors $\mathbf{N}$, when a unit vector $\mathbf{n}$ is well defined. There is an extra solution for zero visibility lines when

$$\mathbf{N} = \sum_\nu w_\nu^B\mathbf{n}_\nu = 0\,. \tag{S.28}$$

This equation can be satisfied only when all vectors **nu** are parallel to each other, i.e. when system A happens to be classical. Then there might be solutions of

$$\sum_\nu (\pm)w_\nu^B = 0\,, \tag{S.29}$$

that define values of parameters (describing system B only) where oscillations vanish.

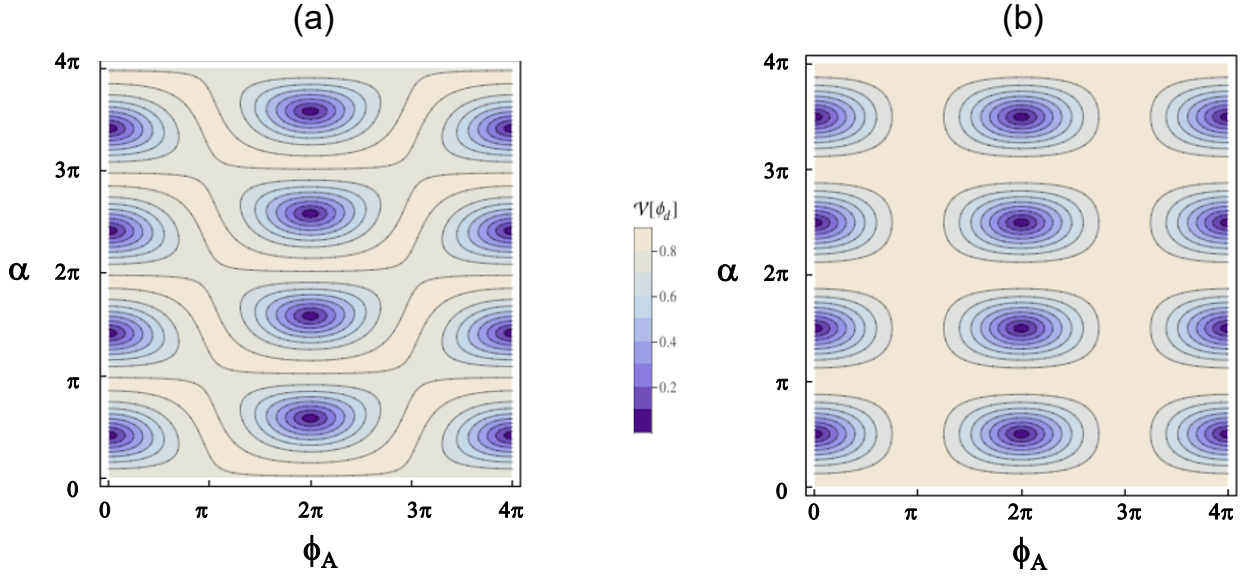FIG. 6. The visibility landscape, Eq. (6), for the two in-states used in Fig. 2 as a function of parameters α and ϕ_A controlling, respectively, the transparency of BS_1^A and the phase difference in MZI^A (see Fig. 1). Here we keep fixed the values of corresponding parameters in MZI^B ($\beta = \pi/3$ and $\phi_B = 0$).

Example: the states with $\phi_\nu = 0$. This corresponds to the configuration when all vectors, $\mathbf{n}_\nu$ and, therefore, $\mathbf{N}$, lie in (x, z)-plane. It is sufficient to consider S_A rotating in that plane only which corresponds to the real $\varphi_\pm = 0$. The amplitude of oscillations becomes

$$\mathcal{A} \sim \mathbf{N}\mathbf{a}_1 = N \sin(\theta - \alpha). \tag{S.30}$$

Generic zeros $\alpha = \theta \bmod \pi$ and extra solutions for classical A-system are found from $w_1^B = w_2^B$ (for two terms case).

Grid-like. In Fig. (5a) the pattern is grid-like which can be observed only for zero-discord system with orthogonal states ρ_ν^A under the extra condition $w_1^B = w_2^B$. For the example used, $w_1^B = (1/10)(1 + \sin\beta)$ and $w_2^B = (4/10)(1 - \sin\beta)$, leading to vertical zero visibility lines at $\sin\beta = 3/5$.

Barcode-like. Zero-visibility lines like those shown in Fig. (5b) again fall into the zero discord category, but without the vertical lines because the states ρ_ν^A are not mutually orthogonal.

Further examples of the protocol

We now further demonstrate how our protocol could be performed in practise. We provide different examples to those given in the main text.

States with no phase differences. This family of states is described by the following density matrix:

$$\rho^{AB} = p \left|\theta_1^A \theta_1^B\right\rangle \left\langle\theta_1^A \theta_1^B\right| + (1 - p) \left|\theta_2^A \theta_2^B\right\rangle \left\langle\theta_2^A \theta_2^B\right|, \tag{S.31}$$

$\Phi_\nu^{A/B}$ is taken to be zero here for simplicity, we will see that little changes in the results of our protocol providing the off-diagonal phase on B are all equal, i.e $\{\Phi_\nu^B\} = \Phi_\nu$. $\{\Phi_\nu^A\}$ will be almost entirely irrelevant as we are concerned only with the A-discord. The protocol of course still works if we do not take the set of Φ_ν^B to be the same for all ν, and we give an example of this later in section .

According to our scheme we now must extract the value of either β_0 or ϕ_{B0} for a fixed α. First, we draw the $\alpha(\phi_A)$ dependence for the state used as the example in the main text (see Fig. (6)).

Next, we arbitrarily choose the value of $\alpha = \pi/3$ and then plot the visibility as a function of β and ϕ_B.

The value of (α_0, ϕ_{A0}) are given by the coordinates where the visibility drops to zero, we only need one of the components, we pick ϕ_{A0} and extract this to be $\phi_{A0} = 0, \pi$ in both cases. We may therefore choose either $\phi_{A0} = 0, \pi$ for the next step. Actually this would be the correct choice for any state within family we have choosen as our
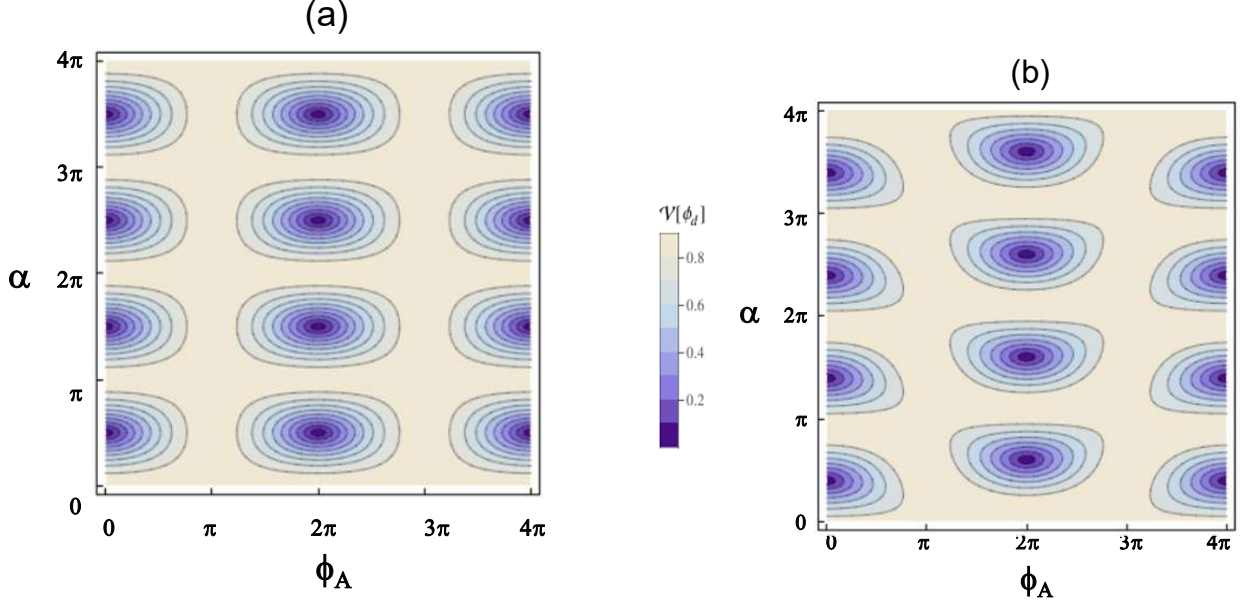
FIG. 7. Visibility as a function of the phase difference of the first loop (ϕ_B) against the varying of BS_1^B (parametrised by β) with α fixed to $\pi/3$. Left: $\rho^{AB} = 1/5\big(|++\rangle\langle++| + 4\,|--\rangle\langle--|\big)$ Right: $\rho^{AB} = 1/2(|\uparrow\uparrow\rangle\langle\uparrow\uparrow| + |\downarrow+\rangle\langle\downarrow+|)$.

examples (given by Eq. (S.31)). The condition $\{\Phi_\nu\} = 0$ reduce to the conditions given by,

$$\tan(\alpha_0) = \pm \frac{\sum_{\nu=1}^n w_\nu^B \sin(\theta_\nu)}{\sum_{\nu=1}^n w_\nu^B \cos(\theta_\nu)}, \qquad\qquad \phi_{A_0} = 0, \pi \qquad\qquad (S.32)$$

where $+, -$ solutions correspond to when $\phi_{A_0} = 0, \pi$ respectively. If we limit ourselves to states which fall within the family of states where $\{\Phi_\nu\} = 0$, then step one of our scheme can be skipped and we can proceed with step two by choosing $\phi_B = 0, \pi$. Similarly, if $\{\Phi_\nu\} = \Phi$ then it can be shown $\phi_{A_0} = \Phi, \Phi + \pi$ in which case we may take $\phi_A = \phi_{A0}$ and skip step 1.

As of yet we can still make no statements about discord, we therefore proceed with step 2 of the protocol; we fix $\phi_{B0} = 0$ (π would have been an equally appropriate choice for our choosen states) and plot the visibility as a function of α, β. This will allow us to extract the equation for β_0,

The graphs clearly display what we expect it to, in the case of zero discord state (left) there are straight horizontal lines of zero visibility corresponding to $\beta_0 = constant$ (note these grid-type graph characteristic of a classically correlated density matrix). Whilst in the second case the lines of zero visibility are clearly α dependent.

The A-discord is sensitive to the states of B-subsystem. We can compare our measure with the discord for a range of density matrices,

$$\rho^{AB} = 1/2\,|\uparrow\uparrow\rangle\langle\uparrow\uparrow| + 1/2\,|\theta^A\theta\rangle\langle\theta^A\theta|\,, \qquad\qquad (S.33)$$

by changing θ^B in the state given by Eq. (S.33) and compare it to Δ_α^2. Discord is plotted for different values of θ^A in Fig. (9) and the complimentary values of Δ_α^2 are given in Fig. 9. We see that, for discord, the peaks of the curves shift and the amplitude is dimished as $\theta^B \to 0$. The peaks of Δ_α^2 also decrease as θ^A is reduced, though the position of the θ-dependent peaks of each function match Fig. (9) less well as θ^A decreases. This measure *always* matches the zeros of discord providing $\{\Phi_{A_\nu}\} = \Phi_A$ however, and thus never produces a false witness in this case.

For $\{\Phi_\nu^A\} \neq \Phi_A$ the measure $\Delta_\alpha^2 > 0$ can fail as a necessary condition for discord some specific states (inspite of the fact our protocol still provides a necessary condition, i.e there will still be no β-independent lines of zero visibility in the $\alpha - \beta$ or $\beta - \phi_A$ visibility landscapes). Therefore if we do not fix $\{\Phi_\nu^A\}$ to a non-zero Δ_α^2 becomes only a sufficient condition for discord. This is a result of some select choices of discorded ρ^{AB} having a α_0 which is not β dependent, but a diagonalising phase, ϕ_{A_0}, which is. In such a situation we may consider a similar function to $f_\alpha(\beta)$ but based on ϕ_{A_0} as opposed to α_0 we consider,

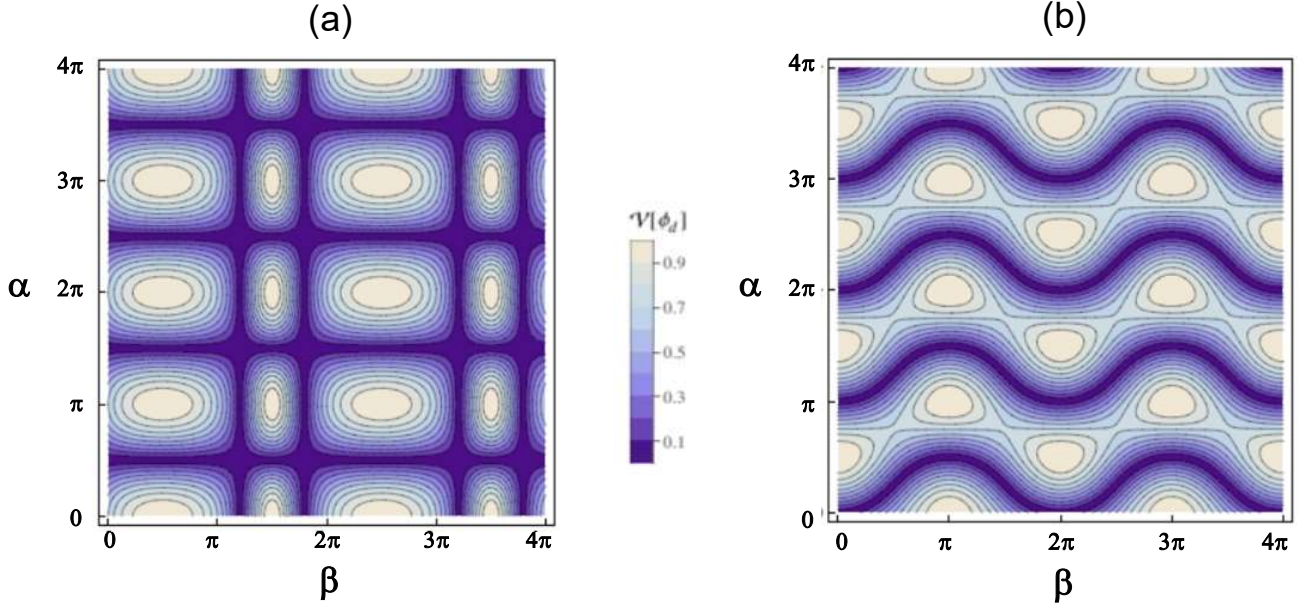$$f_\phi(\beta) \equiv \cos^2(\phi_{A_0}) = \mathcal{N}_x^2/(\mathcal{N}_x^2 + \mathcal{N}_y^2) \qquad\qquad (S.34)$$

FIG. 8. Visibility as a function of α and β with $\phi_A = \phi_{A_0}$. (a): $\rho^{AB} = 1/5\,|++\rangle\langle++| + 4/5\,|--\rangle\langle--|$ (b): $\rho^{AB} = 1/2\,|\uparrow\uparrow\rangle\langle\uparrow\uparrow| + 1/2\,|+\downarrow\rangle\langle+\downarrow|$.

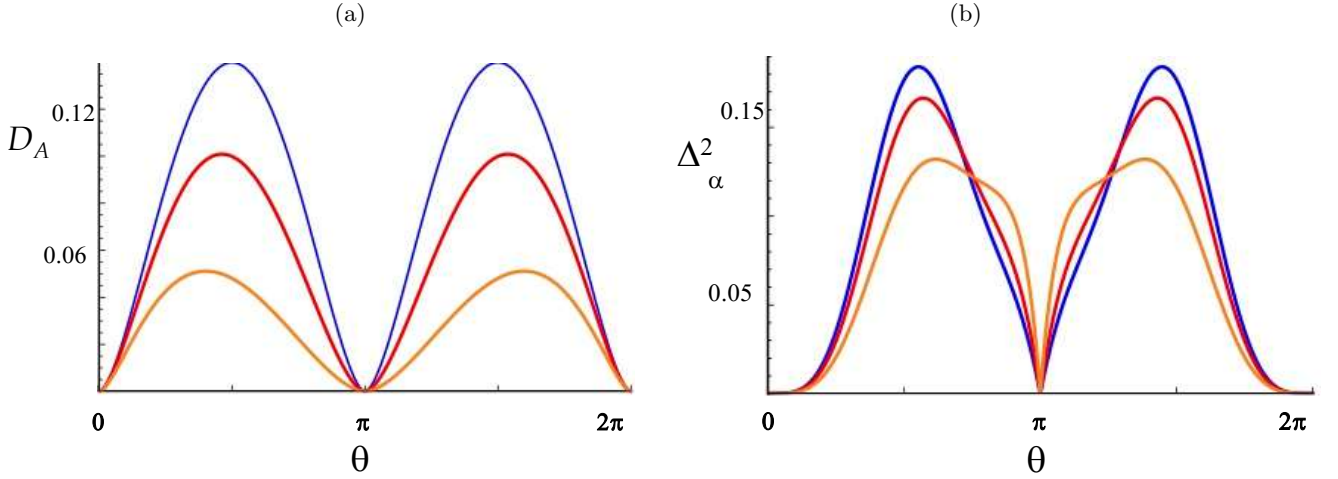FIG. 9. Discord (a) and our quantifier Δ_α^2 (b) for state Eq. (S.33) with, $\theta^A = \pi$ (blue), $\theta^A = \pi/2$ (red), $\theta^A = \pi/4$ (orange).

We may then consider the standard deviation of this quantity Δ_ϕ^2 (defined similarly to Eq. (7)) which, when it is > 0, also individually provides a sufficient condition for discord. Together with Δ_α^2, however, it provides a necessary condition, i.e $\Delta_\phi^2 + \Delta_\alpha^2 > 0$ is a necessary condition for discord. We give an example where Δ_α^2 on it own fails as a witness in the next section, but see even with being the case that it is clear from the $\alpha - \beta$-visiblity landscape whether the state is discorded or not.

States with phase differences. Up until this point we only considered examples of our protocol for when density matrices ρ_ν^A had the same off-diagonal phase, but our protocol also works for states where the phases are different. Below we will give an example of what we would expect using our protocol for a state with off-diagonal phase on A, we will continue to assume there is no off-diagonal phase on B for the sake of simplicity. We consider the state,

$$\rho^{AB} = \frac{1}{2}\,|+;+,\Phi_1\rangle\langle+;+,\Phi_1| + \frac{1}{2}\,|-;-,\Phi_2\rangle\langle-;-,\Phi_2| \tag{S.35}$$

where $|\theta_{A_\nu};\theta_{B_\nu},\Phi_{B_\nu}\rangle \equiv |\theta_{A_\nu}\rangle \otimes |\theta_{B_\nu},\Phi_{B_\nu}\rangle \equiv |A_\nu\rangle\big|_{\Phi_{A_\nu}=0} \otimes |B_\nu\rangle$. The above state has zero discord providing that $\Phi_1 = \Phi_2 + n\pi$ where n is an integer. We will arbitrarily pick $\Phi_1 = 0$ and $\Phi_2 = \pi/2$ so that the resulting state is discorded and then proceed to check this using our protocol. First we plot the visibility graph with fixed β (we choose
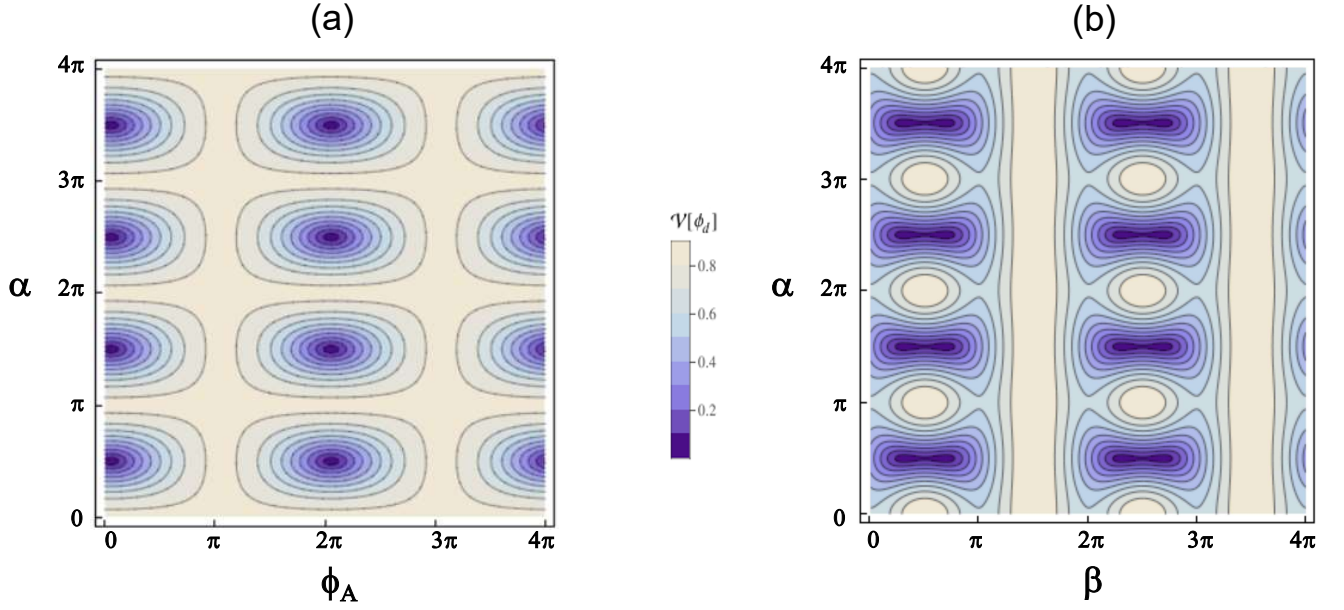
(a)

(b)

FIG. 10. The visibility plots for the density matrix given by Eq. (S.35 with $\Phi_1 = 0$ and $\Phi_2 = \pi/2$, (a) Shows visibility as function of α, ϕ_A with $\beta = 2\pi/3$, (b) gives visibility plot as function of α, β now fixing $\phi_A = \arctan\left(\frac{2-\sqrt{3}}{3}\right)$ (see Eq. (S.36).

(b)
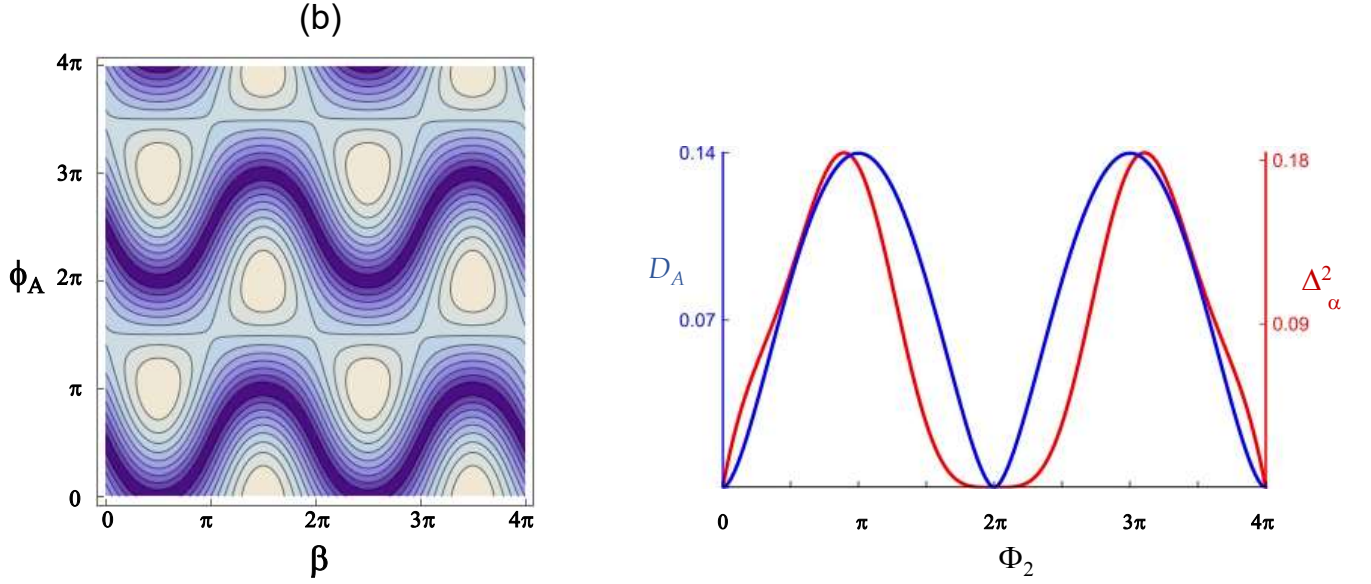

FIG. 11. (a) Visibility plot for the density matrix given by Eq. (S.35 with $\Phi_1 = 0$ and $\Phi_2 = \pi$, plots are given as a function of ϕ_A and α with $\beta = \beta_0 = \pi/2$. (b) demonstrates discord and Δ_ϕ^2 for the state described by Eq. (S.35 for a range of Φ_2 with $\Phi_1 = 0$.

$\beta = 2\pi/3$) as function of α and ϕ_A, this is shown in Fig. (10a). These graphs appear similar to the ones shown earlier, but the values of ϕ_A where visibility drops to zero are now slightly shifted from zero and π. Their positions are given by,

$$\phi_{A0} = \arctan\left(\frac{2-\sqrt{3}}{3}\right) \quad \mod \quad \pi. \tag{S.36}$$

Fixing ϕ_A to the first of these values we then plot the visibility as a function of α and β, this is given in (10b).

The difference between the state shown here and those given previously is now apparent. It is even more stark here that the parameters α_0, ϕ_{A0} depend on β. This is due to the fact the value of ϕ_{A0} is now also β-dependent (in previous examples where $\{\Phi_\nu\} = \Phi$ it was only α_0 which depended on β). This means that as β is changed we no

longer have the correct value of ϕ_A which diagonalises the state, and since to diagonalise the state both $\alpha = \alpha_0$ and $\phi_A = \phi_{A0}$ must be true there are large regions of Fig. 11(b) where the state can not be diagonalised and therefore visibility can not go to zero. A very clear demonstration that the state is discorded. This is an example of where if we take Δ_α^2 alone we would not be able to tell the state were discorded (in spite of how obvious it is from the Fig. 10(b)), Δ_ϕ^2 however behaves similarly to discord as seen in Fig. 11(b). Δ_ϕ^2 may be extracted from visibility landscapes like Fig. 11(a) in which α is fixed to α_0 and we have plotted the visibility as a function of ϕ_A and β.

Example with three states. We have previously limited ourselves to examples with $n = 2$ in a separable density matrix described by Eq. (1), we briefly consider an example with $n = 3$,

$$\rho^{AB} = 1/3 \,|\uparrow\uparrow\rangle \langle\uparrow\uparrow| + 1/3 \,|\downarrow\downarrow\rangle \langle\downarrow\downarrow| + 1/3 \,|\theta\theta\rangle \langle\theta\theta| \tag{S.37}$$

Since the state is real we know that the correct choice of the diagonalising rotation is $\phi_{A_0} = 0$, fixing ϕ_A to this value we can then plot the visibility as a function α and β, Fig (12a) gives a snapshot of one of these visibility graphs for $\theta = \pi/2$. We see the characteristic waviness which correctly tells us the state is discorded, Δ_α^2 for this value of θ can be extracted from this graph. We plot Δ_ϕ^2 for different θ and contrast it to A-discord in Fig. (12b). We see that once again the most important features of discord are mirrored in Δ_ϕ^2.
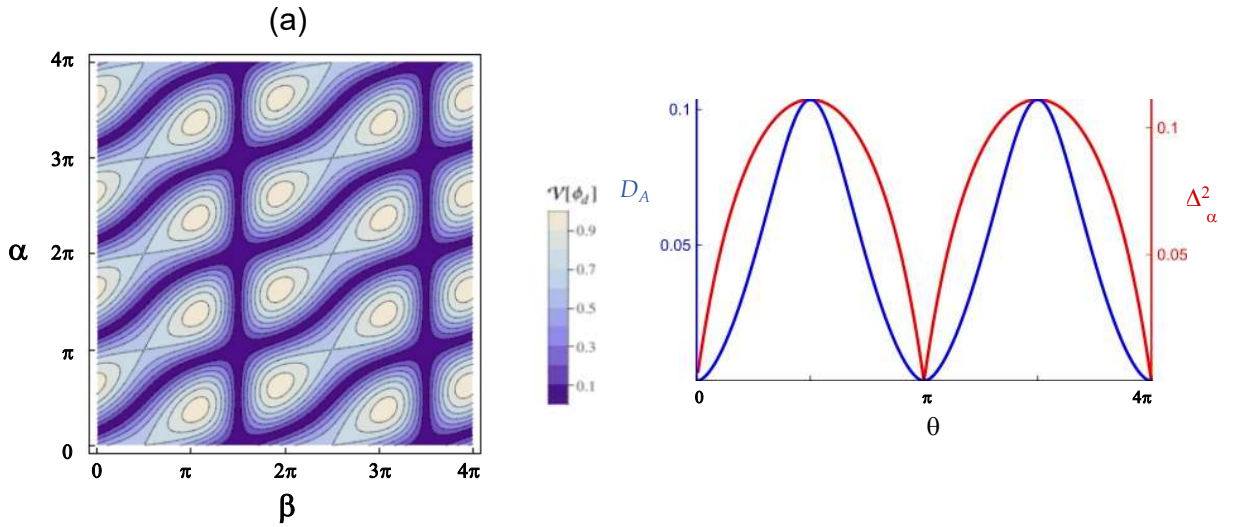

FIG. 12. (a) Shows a visibility plot of density matrix given by Eq. (S.37) with $\theta = \pi/2$, the tell-tale signs of discord are present in the curviness of the zero-visibility lines. (b) plots the discord of Eq. (S.37) for different θ and contrasts it to the measure of curviness which can be extracted from graphs like that shown in (a).

Experimentally obtaining measure for 3D lines of zero visibility. In order to experimentally obtain $\Delta_\alpha^2 + \Delta_\phi^2$ for a completely general state, one considers the full zero-visibility lines in three-dimensional space (α, β, ϕ_A). The discord quantifier is extracted from this line by calculating $\Delta_\alpha^2 + \Delta_\phi^2 0$, which is zero only if discord is absent. The measures Δ_α^2 and Δ_ϕ^2 can be obtained by the projection of the line onto the $\alpha - \beta$ and $\phi_A - \beta$ planes respectively.

———

[1] H. Ollivier and W. H. Zurek, Phys. Rev. Lett. **88**, 017901 (2001).
[2] L. Henderson and V. Vedral, J. Phys. A **34**, 6899 (2001).
[3] V. Vedral, arXiv:quant-ph , 1702.01327 (2017).
[4] B. Dakić, V. Vedral, and C. Brukner, Phys. Rev. Lett. **105**, 190502 (2010).
[5] A. Ferraro, L. Aolita, D. Cavalcanti, F. M. Cucchietti, and A. Acín, Phys. Rev. A **81**, 052318 (2010).
[6] K. Modi, A. Brodutch, H. Cable, T. Paterek, and V. Vedral, Rev. Mod. Phys. **84**, 1655 (2012).